Constraints on Hidden Photons Produced in Nuclear Reactors

Mikhail Danilov,[1,*] Sergey Demidov,[2,3,†] and Dmitry Gorbunov[2,3,‡]

[1]*Lebedev Physical Institute of the Russian Academy of Sciences, Moscow 119991, Russia*
[2]*Institute for Nuclear Research of the Russian Academy of Sciences, Moscow 117312, Russia*
[3]*Moscow Institute of Physics and Technology, Dolgoprudny 141700, Russia*

New light vector particles—hidden photons—are present in many extensions of the standard model of particle physics. They can be produced in nuclear reactors and registered by neutrino detectors. We obtain new limits on the models with the hidden photons from an analysis of published results of the TEXONO neutrino experiment. Accounting for oscillations between the visible and hidden photons, we find that the neutrino experiments are generally insensitive to the hidden photons lighter than ~ 0.1 eV.

A number of extensions of the standard model of particle physics (SM) introduce massive vectors, singlet with respect to the SM gauge group. These hypothetical particles are called hidden photons, dark photons, or paraphotons [1]. They can serve as dark matter particles or messengers between the visible sector (SM) and hidden sector(s). Dynamics of the latter solves (some of) the SM phenomenological and theoretical problems (neutrino oscillations, matter-antimatter asymmetry of the Universe, etc.) or suggests some phenomena that impacts on physics and the Universe, which are not recognizable at present (see, e.g., Refs. [2–4]).

The hidden photon can couple to the SM via vector portal interaction. The corresponding coupling constant is dimensionless, and hence low- and high-energy experiments exhibit similar sensitivity to this type of new physics, if the hidden photon is sufficiently light. In particular, the hidden photon X_μ of mass m_X can mix with the SM photon A_μ, the relevant Lagrangian [5] reads

$$\mathcal{L} = -\frac{1}{4}F_{\mu\nu}^2 - \frac{1}{4}X_{\mu\nu}^2 - \frac{\epsilon}{2}X_{\mu\nu}F^{\mu\nu} + \frac{m_X^2}{2}X_\mu^2 - eA_\mu j_{em}^\mu. \quad (1)$$

Here $F_{\mu\nu} \equiv \partial_\mu A_\nu - \partial_\nu A_\mu$, $X_{\mu\nu} \equiv \partial_\mu X_\nu - \partial_\nu X_\mu$; ϵ is a dimensionless parameter of visible-hidden photon mixing and j_{em}^μ is electromagnetic current.

The mixing term in Eq. (1) can be responsible for the hidden photon production in a nuclear reactor, if kinematically allowed; hidden photons of, i.e., $m_X \lesssim 1$ MeV can be produced by photons of energy $E_\gamma \sim 1$–10 MeV.

For sufficiently small m_X, the mixing in Eq. (1) converts photons into hidden photons via oscillations similar to the well-studied neutrino oscillations. The visible-to-hidden photon oscillations are fully described, e.g., in Ref. [6], which is devoted to the hidden photon production and propagation in the Sun. Given the above analogy with neutrino oscillations, we consider the interaction eigenstates to be more convenient for the estimate of hidden photon yield. Typically, one replaces (see, e.g., Ref. [7]) the hidden photon in Eq. (1) as $X_\mu \to S_\mu - \epsilon A_\mu$, with S_μ being sterile with respect to the electromagnetic interaction. The kinetic term of Eq. (1) becomes diagonal in terms of the new variables, while the mass term gains off-diagonal components. The interaction with the electromagnetic current produces a quantum wave packet of photon A_μ, which is not a propagation eigenstate. In the relativistic regime, the evolution of transverse modes of the photon–hidden photon system can be described by the following Hamiltonian (see, e.g., Ref. [8])

$$H = \frac{1}{2E_\gamma}\begin{pmatrix} \epsilon^2 m_X^2 + m_\gamma^2 & -\epsilon m_X^2 \\ -\epsilon m_X^2 & m_X^2 \end{pmatrix}. \quad (2)$$

Here m_γ is an effective mass of the photon which the latter acquires due to its coherent forward scattering off free electrons of the media [9]. The value of m_γ coincides with the corresponding plasma frequency [10], $m_\gamma^2 = 4\pi\alpha n_e/m_e$, where α is fine-structure constant, m_e is electron mass, and n_e is density of free electrons (for the reactor photon energies, all electrons in matter can be considered as free) inside the reactor. Numerically, for the reactor material, one finds that the photon mass varies within

$$m_\gamma \simeq 20\text{–}60 \text{ eV}. \quad (3)$$

The Hamiltonian (2) determines the propagation eigenstates of the system, which are mixtures of A_μ and S_μ. In terms of

interaction eigenstates S_μ and A_μ, their evolution looks like oscillations, with the transition probability $P(\gamma \to \gamma') = 4\epsilon^2 \sin^2(\Delta m^2 L/4E_\gamma)$ valid for negligible absorption. The corresponding oscillation length is given by

$$L_{\text{osc}} \approx 2.5 \text{ cm} \times \frac{E_\gamma}{1 \text{ MeV}} \frac{(10 \text{ eV})^2}{\Delta m^2}, \qquad (4)$$

where the mass squared difference Δm^2 reads

$$\Delta m^2 = \sqrt{(m_X^2 - m_\gamma^2)^2 + 2\epsilon^2 m_X^2 (m_X^2 + m_\gamma^2)}. \qquad (5)$$

The latter never falls below $m_\gamma^2 \gtrsim (20 \text{ eV})^2$, except for the region, $m_X \approx m_\gamma$, where the oscillation length [Eq. (4)] is largest, and which we call the resonance region in what follows. Hence, the oscillation length [Eq. (4)] is typically much smaller than the size of the nuclear reactor core of order meters.

The oscillations between the states S_μ and A_μ proceed until the corresponding wave packets of the Hamiltonian eigenstates get separated in space due to their different velocities, or photon interacts in media; both processes naturally break the quantum coherence between the two oscillating states and invalidate the oscillation approximation to the hidden photon production. The relevant coherence length due to space separation of wave packets in vacuum can be estimated as $l_{\text{coh}} \sim \sigma/\Delta v$ where σ is size of the photon wave packet at production and Δv is difference in velocities of the mass eigenstates. Using typical half-lifes of prompt γ decays of fission fragments about 10^{-12}–10^{-11} s (see, e.g., Refs. [11,12]), one obtains $\sigma \sim 0.03$–0.3 cm. The corresponding coherence length $l_{\text{coh}} \sim 6 \times 10^{8-9} \text{ cm} \times (E_\gamma/1 \text{ MeV})^2 (10 \text{ eV})^2/\Delta m^2$ always exceeds the oscillation length [Eq. (4)]. This statement remains true even in the media where the coherence length decreases due to interactions of fission products and after the rescattering of photons off electrons reducing σ to 10^{-6} cm. So the oscillation approximation is justified in our case.

The oscillation is terminated by absorption of the photon in the reactor material. The photon absorption length in a nuclear reactor, $1/\Gamma$, varies from a few to few tens cm for the energy range 1–10 MeV. Its effect can be described by the replacement $(m_\gamma^2/2E_\gamma) \to (m_\gamma^2/2E_\gamma) - i\Gamma$ in the Hamiltonian [Eq. (2)]. The absorption length is much shorter than the reactor size of about several meters, but it is typically longer than the oscillation length [Eq. (4)] except for the resonance region $\Delta m^2 \approx 0$. In the following numerical estimates, we take $1/\Gamma = 10$ cm. Most photons produced in the core get absorbed in the reactor material (mostly in water and steel) unless they oscillate into hidden photons with the probability [6]

$$P = \epsilon^2 \times \frac{m_X^4}{(\Delta m^2)^2 + E_\gamma^2 \Gamma^2}, \qquad (6)$$

which can be obtained straightforwardly by solving the Schrodinger equation with the Hamiltonian [Eq. (2)] for distances larger than the absorption length. The terms in the denominator of Eq. (6) are responsible for the photon absorption dominates when

$$\Delta m^2 \ll E_\gamma \Gamma \approx 2 \times \left(\frac{E_\gamma}{1 \text{ MeV}}\right)\left(\frac{10 \text{ cm}}{1/\Gamma}\right) \text{ eV}^2, \qquad (7)$$

i.e., in the resonance region, where $m_X \approx m_\gamma$ with the accuracy of a few percent.

In the nonresonance case, the condition [Eq. (7)] is opposite, and the probability depends on the relation between m_X and m_γ. For heavier hidden photons, i.e., when $m_X \gg m_\gamma > 20$ eV, the probability turns to simple $P = \epsilon^2$ law. In the absence of coherence in a γ-X system, this result follows from the calculation of Compton scattering with X emerging due to mixing with photon. This result deviates from that in Ref. [13], where a numerical factor $2/3$ was introduced to account for difference in numbers of polarization states between photon (two) and massive photon (three). We find this factor irrelevant since only two transverse polarizations of the hidden photon are produced via oscillations of the massless photon. The production of the longitudinal component of the massive photon is suppressed for the masses and photon energies of interest, $P \propto m_X^2/E_\gamma^2$ (see, e.g., Refs. [8,14]). In the opposite case, $m_X \ll m_\gamma$, one obtains from Eq. (6) the following:

$$P \approx 6 \times 10^{-6} \times \epsilon^2 \times \left(\frac{m_X}{1 \text{ eV}}\right)^4, \qquad (8)$$

where we use $m_\gamma = 20$ eV for the estimate.

The hidden photon production rate is obtained by convolution of the probability [Eq. (6)] with the photon flux in the reactor, which we take normalized to that measured [15] for $E_\gamma \gtrsim 0.2$ MeV from the FRJ-1 reactor core

$$\frac{dN_\gamma}{dE_\gamma} = 0.58 \times 10^{21} \times \frac{T}{\text{GW}} \times e^{-(E_\gamma/0.91 \text{ MeV})}$$

in units photons/(s MeV), with T being the reactor thermal power. The hidden photons leave the reactor and can be observed at some distance in a detector designed to measure the reactor antineutrino flux. The hidden photons oscillate and produce photons, which can be detected via the Compton scattering of electrons. Each hidden photon then produces the Compton-like signature with the probability

$$P = \epsilon^2 \times \frac{m_X^4}{(\Delta m^2)^2}, \tag{9}$$

[see Eq. (6), where we set $\Gamma = 0$, which can be done away from the resonance region] and m_γ in Δm^2; Eq. (5) should be calculated for material along the hidden photon path inside the detector. Even neglecting m_γ (that is, for $m_X \gg m_\gamma$), one obtains an estimate $P \approx \epsilon^2$.

However, the neutrino detectors are made of dense material, so the effective photon mass is certainly not smaller than that in water. For the numerical estimates below, we chose $m_\gamma = 20$ eV inside neutrino detector as well. Hence, the total probability in a general nonresonance case is just a product of Eqs. (6) and (9), which implies a huge suppression factor for the light hidden photons, $m_X \ll m_\gamma$.

In the resonance case, $m_\gamma = m_X$, the mass difference [Eq. (5)] becomes equal to

$$\Delta m^2 = 0.8 \times \frac{\epsilon}{10^{-3}} \left(\frac{m_\gamma}{20 \text{ eV}} \right)^2 \text{ eV}^2,$$

and the oscillation length [Eq. (4)] is

$$L_{\text{osc}} = 3 \text{ m} \frac{E_\gamma}{1 \text{ MeV}} \frac{10^{-3}}{\epsilon} \left(\frac{20 \text{ eV}}{m_\gamma} \right)^2.$$

One observes, that, for the $\epsilon < 10^{-3}$ condition, Eq. (7) is obeyed and the probability [Eq. (6)] reduces to

$$P \approx 4 \times 10^4 \times \epsilon^2 \times \left(\frac{m_\gamma}{20 \text{ eV}} \right)^4 \times \left(\frac{1 \text{ MeV}}{E_\gamma} \right)^2. \tag{10}$$

One expects a similar enhancement for the hidden-to-visible conversion probability; however it generally occurs for another resonance mass m_X, since the reactor and detector materials are different, as well as the corresponding photon masses.

Therefore, in the two very narrow mass ranges, the number of signal events in the detector gets amplified a hundred thousand times with respect to the Compton-based result, $P = \epsilon^2$. Since the estimate [Eq. (10)] is valid only in the very narrow mass ranges defined by the photon effective mass in the matter, its applicability requires a good knowledge of the nuclear reactor core structure and the detector, which is unavailable for us. However, it can be applied by, e.g., the NEOS and TEXONO collaborations. Note that, in the realistic case of inhomogeneous materials, the probability formula [Eq. (6)] gets modified (see Ref. [6]).

A side remark concerns the recent letter [13] where a study similar to ours was performed, but the oscillations were neglected. We find that at $m_X \gtrsim 20$ eV its results for the event numbers are underestimated by factor 3/2, except the resonance regions where they may be (a special study is

needed) underestimated by a factor of $\sim 10^5$. For lighter hidden photons, $m_X \lesssim 20$ eV, the number of signal events are overestimated by factor $2/3 \times (m_\gamma/m_X)^8$, see expressions for the conversion probabilities [Eqs. (6) and (9)]. While Ref. [13] claims the mass-independent upper limit of about $\epsilon \lesssim 10^{-5}$, our observation suggests, instead, that the neutrino experiments are absolutely insensitive to the hidden photons lighter than about 0.05 eV.

Now we turn to the analysis of the experimental data of the TEXONO neutrino experiment [16], and use its result to place limits on mixing ϵ (see Ref. [17] for a similar study in a model where a new massive vector boson directly couples to neutrinos). To measure the $\bar{\nu}_e - e^-$ scattering cross section, the TEXONO experiment used a scintillator crystal detector, located at 28 m from the core of a $T = 2.9$ GW thermal-power reactor. With electron recoil energy in the 3–8 MeV range, the TEXONO collaboration extracted 414 ± 100.6 events in 160 days. This number is 30.7 ± 100.6 events larger than the SM expectation. The excess is smaller than 195.7 events at the 95% C.L. We use this number to determine the 95% C.L. upper limit on the number of hidden photons detected in the TEXONO experiment. The TEXONO collaboration applies a special anti-Compton selection, which reduces the background by a factor of 6 in the energy range 3–8 MeV utilized for the searches. The signature of a hidden photon is identical to the Compton scattering process. Therefore, the anti-Compton selection decreases the efficiency of the hidden photon detection. The suppression factor of the anti-Compton selection for single photons is not given by the TEXONO collaboration. It can be smaller than that for the background suppression. However, for the upper limit estimates we can assume them to be equal. This leads to the upper limit of 1174.1 hidden photon events in the TEXONO experiment at the 95% C.L.

In Fig. 1 we present a revised 95% C.L. upper limit on the parameters ϵ and m_X of the model from TEXONO data where, in recalculation of the results from Ref. [13], we take into account both the theoretical and experimental issues discussed above. At large masses of the hidden photon, i.e., $m_X \gtrsim 20$ eV, the overall correction to the signal estimate claimed in Ref. [13] is a factor of 4; given the ϵ^4 dependence, the corresponding limit on ϵ is only slightly weaker than that presented in Ref. [13]. At the same time we see that the sensitivity of the reactor experiment to the hidden photon model is drastically decreased for $m_X \lesssim 20$ eV.

A side remark concerns Ref. [13], where TEXONO and NEOS data were both analyzed to constrain ϵ. For the TEXONO data analysis in Ref. [13] the suppression of the hidden photon detection efficiency due to the anti-Compton selection was ignored. This underestimates the upper limit on the number of hidden photons by a factor that can be as large as 6. Analysis of the NEOS data is wrong at several points. Since Ref. [23] from Ref. [13] is not available to us, we naturally assume that the conclusion that "all of the
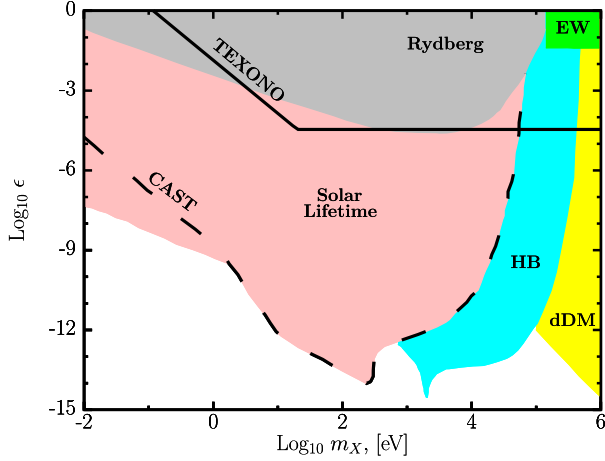
FIG. 1. 95% C.L. exclusion upper limit in the parameter plane (m_X, ϵ) of the hidden photon model from TEXONO experiment (black solid line) in comparison with other results (see Ref. [18] for details).

reactor-on event candidates are due to background" is based on the approximate equality $N_{\rm on}/T_{\rm on} = N_{\rm off}/T_{\rm off}$. Here $N_{\rm on}$ ($N_{\rm off}$) and $T_{\rm on}$ ($T_{\rm off}$) are the number of e/γ events and data taking time during the reactor on (off) period. Then the absence of the signal events associated with the hidden photons implies

$$N_{\rm hph} = N_{\rm on} - N_{\rm off} \frac{T_{\rm on}}{T_{\rm off}} \approx 0. \qquad (11)$$

Its statistical uncertainty,

$$\Delta N_{\rm hph} = \sqrt{N_{\rm on} + N_{\rm off} \frac{T_{\rm on}^2}{T_{\rm off}^2}} = \sqrt{N_{\rm on} \left(1 + \frac{T_{\rm on}}{T_{\rm off}}\right)},$$

determines the upper limit on the hidden-visible mixing, $1.64 \Delta N_{\rm hph}$ would correspond to 95% C.L. It is worth to mention that the two-sided C.L. were used in Ref. [13] instead of a one-sided C.L. Therefore, the obtained upper limits correspond to 97.5% C.L. instead of 95% C.L. Numerically, for the NEOS on- and off-time intervals, we obtain $\Delta N_{\rm php} \approx 2.2 \times \sqrt{N_{\rm on}}$ instead of $\sqrt{N_{\rm on}}$ adopted in Ref. [13].

Even more important is that the estimation of the upper limit ignores possible systematic errors. The upper limit corresponds to 7.3×10^{-5} of the total number of e/γ events. This small number implicitly assumes the absence of time variations of the detector efficiency and background contribution at a similar very low relative level. The NEOS experiment [19] has not presented any evidence of such a challenging stability.

Indeed, signatures of the hidden photon interactions in the NEOS detector are practically indistinguishable from signatures of positrons in the electron antineutrino induced

inverse beta decay (IBD) reactions. The NEOS experiment detected 339.1 thousand IBD events whose signature includes a part from a prompt positron signal as well as a delayed event resulting from n-Gd capture. At least 292.7 thousand of them (1626 events per day during the 180 days of data taking) had the total positron energy (prompt energy) in the range 1–5 MeV, at which the estimation of the expected number of hidden photons was performed. This number is 5.5 times larger than the 95% C.L. upper limit on a number of observed hidden photon events presented in Ref. [13]. Here we again point out that the hidden photon event candidates would look like single prompt events, and thus their number cannot be smaller than the number of fully reconstructed IBD events divided by the neutron detection efficiency and other IBD process selection efficiencies. This observation again explicitly demonstrates that the estimation [13] of the upper limit on the number of detected hidden photons in the NEOS experiment cannot be correct. It is a factor of 6 too optimistic. For a typical stability of the detector efficiency and background level of about 1%, the limit on the number of the detected hidden photons in the NEOS experiment derived in Ref. [13] is 2 orders of magnitude too optimistic. That is why we do not use the NEOS data in our calculations of the upper limit on the mixing parameter ϵ shown in Fig. 1.

To conclude, we present theoretical description of the expected dark photon signal in reactor neutrino experiments and obtain corrected upper limits on the hidden photon mass m_X and the mixing parameter ϵ from the TEXONO data, see Fig. 1. There are two comments in order. First, we disregard the Compton rescattering of the photons during their propagation in the reactor core. The secondary photons may contribute to the hidden photon production. In this respect, our limits are conservative. Second, in our estimates, we take the minimum value of the effective photon mass equal $m_\gamma \approx 20$ eV for the reactor and detector. The sensitivity to lighter hidden photons, $m_X < m_\gamma$, is strongly reduced. The chosen value refers to water and grows in denser materials, thus suppressing the sensitivity for correspondingly heavier hidden photons. Therefore, we expect, that limits in Fig. 1 may be improved, but only mildly, with dedicated analyses performed by the NEOS and TEXONO collaborations. The only promising case is the resonance, $m_X \approx m_\gamma$, where the amplified production of the hidden photons may significantly improve the limit on mixing ϵ.

*mvdanil@gmail.com
†demidov@ms2.inr.ac.ru
‡gorby@ms2.inr.ac.ru

[1] L. B. Okun, Sov. Phys. J. Exp. Theor. Phys. **56**, 502 (1982) [Zh. Eksp. Teor. Fiz. **83**, 892 (1982)].

[2] M. Pospelov, A. Ritz, and M. B. Voloshin, Phys. Lett. B **662**, 53 (2008).

[3] J. D. Bjorken, R. Essig, P. Schuster, and N. Toro, Phys. Rev. D **80**, 075018 (2009).

[4] P. Ilten, Y. Soreq, M. Williams, and W. Xue, J. High Energy Phys. 06 (2018) 004.

[5] B. Holdom, Phys. Lett. **166B**, 196 (1986).

[6] J. Redondo, J. Cosmol. Astropart. Phys. 07 (2015) 024.

[7] J. Redondo, J. Cosmol. Astropart. Phys. 07 (2008) 008.

[8] J. Redondo and G. Raffelt, J. Cosmol. Astropart. Phys. 08 (2013) 034.

[9] E. Braaten and D. Segel, Phys. Rev. D **48**, 1478 (1993).

[10] E. Lifshitz and L. Pitaevski, *Course of Theoretical Physics* (Pergamon, Amsterdam, 1981), vol. 10.

[11] S. A. Johansson, Nucl. Phys. **60**, 378 (1964).

[12] H. Albinsson, Phys. Scr. **3**, 113 (1971).

[13] H. Park, Phys. Rev. Lett. **119**, 081801 (2017).

[14] H. An, M. Pospelov, and J. Pradler, Phys. Lett. B **725**, 190 (2013).

[15] H. Bechteler *et al.*, Spez. Ber. Kernforschungsanlage Juelich **255**, 62 (1984).

[16] M. Deniz *et al.* (TEXONO Collaboration), Phys. Rev. D **81**, 072001 (2010).

[17] M. Lindner, F. S. Queiroz, W. Rodejohann, and X.-J. Xu, J. High Energy Phys. 05 (2018) 098.

[18] J. Jaeckel and A. Ringwald, Annu. Rev. Nucl. Part. Sci. **60**, 405 (2010).

[19] Y. J. Ko, B. R. Kim, J. Y. Kim, B. Y. Han, C. H. Jang, E. J. Jeon, K. K. Joo, H. J. Kim, H. S. Kim, Y. D. Kim, J. Lee, J. Y. Lee, M. H. Lee, Y. M. Oh, H. K. Park, H. S. Park, K. S. Park, K. M. Seo, K. Siyeon, and G. M. Sun (NEOS Collaboration), Phys. Rev. Lett. **118**, 121802 (2017).